









Development of nano-antimicrobial material based on bacterial cellulose, silver nanoparticles, and ClavaninA

Glícia Maria Oliveira¹ , Alberto Galdino Silva-Junior^{1,2} , Octávio Luiz Franco³ ,
José Lamartine de Andrade Aguiar⁴ , Flávia Cristina Morone Pinto⁴ ,
Reginaldo Gonçalves de Lima-Neto⁵ , Maria Danielly Lima de Oliveira^{1,2} ,
and César Augusto Souza de Andrade^{1,2*} 

¹Programa de Pós-graduação em Inovação Terapêutica, Universidade Federal de Pernambuco – UFPE, Recife, PE, Brasil

²Laboratório de Biodispositivos Nanoestruturados, Departamento de Bioquímica, Universidade Federal de Pernambuco – UFPE, Recife, PE, Brasil

³Programa de Pós-graduação em Ciências Genômicas e Biotecnologia, Centro de Análises Proteômicas e Bioquímica de Brasília, Universidade Católica de Brasília – UCB, Brasília, DF, Brasil

⁴Programa de Pós-graduação em Cirurgia, Departamento de Cirurgia, Universidade Federal de Pernambuco – UFPE, Recife, PE, Brasil

⁵Laboratório de Pesquisa e Diagnóstico em Doenças Tropicais, Centro de Ciências Médicas, Universidade Federal de Pernambuco – UFPE, Recife, PE, Brasil

*csrandrade@gmail.com

Abstract

This study presents a novel approach to obtaining nano-antimicrobial hybrid material by integrating electrospun nanofibers based on cellulosic biopolymer (BP) associated with antimicrobial agents, specifically silver nanoparticles (AgNPs) and Clavanin A (ClavA), an antimicrobial peptide obtained from the marine tunicate *Styela clava*. The electrospinning technique produced the blended polyvinyl alcohol:BP nanofibers. Chemical crosslinking was performed to ensure the stability of the nanofibers. The nanofibers had an average diameter of 568 nm for PVA nanofibers and 648 nm for PVA nanofibers functionalized with silver nanoparticles. The nanohybrid material demonstrates significant inhibition zones against Gram-positive (*Bacillus subtilis*, *Staphylococcus aureus*) and Gram-negative (*Pseudomonas aeruginosa*, *Klebsiella pneumoniae*) bacteria. *P. aeruginosa* exhibits a substantial inhibition zone of 15 mm. Thus, the nanohybrid material was effective against this challenging pathogen. Combining electrospun nanofibers, bacterial cellulose hydrogel, and antimicrobial agents establishes a solution that could combat microbial threats in wound care.

Keywords: antimicrobial peptide, Clavanin A, electrospinning, silver nanoparticles, sugarcane biopolymer.

How to cite: Oliveira, G. M., Silva-Junior, A. G., Franco, O. L., Aguiar, J. L. A., Pinto, F. C. M., Lima-Neto, R. G., Oliveira, M. D. L., & Andrade, C. A. S. (2024). Development of nano-antimicrobial material based on bacterial cellulose, silver nanoparticles, and ClavaninA. *Polímeros: Ciência e Tecnologia*, 34(3), e20240030. <https://doi.org/10.1590/0104-1428.20240029>

1. Introduction

Chronic or acute wounds create a conducive environment for microbial colonization, posing a severe threat to healing processes. Microorganisms in wounds amplify the risk of infections, complicating treatment and potentially leading to systemic issues^[1]. The increase in healthcare expenditures arises from the need for specialized wound care, antibiotics, and surgical interventions^[2]. Chronic wounds demand prolonged treatment, escalating healthcare costs and contributing to productivity losses as individuals grapple with persistent health challenges. Additionally, the economic impact is related to increased antibiotic resistance, requiring more resources for research and development of alternative treatments^[3]. Effectively managing wound-related microbial issues is

imperative for the public health and alleviating the strain on healthcare systems and global economies^[2].

Current wound dressings, while effective, often face limitations in addressing diverse wound types and promoting optimal healing. Traditional dressings may lack specificity in managing infections, controlling inflammation, or facilitating tissue regeneration^[4]. The need for new alternatives stems from the increasing prevalence of complex wounds, such as chronic ulcers and traumatic injuries, which demand advanced materials and technologies for personalized care. Innovative wound dressings, incorporating bioactive compounds, nanomaterials, and smart polymers, are essential to enhance therapeutic outcomes, reduce healing time, and

minimize the economic burden associated with prolonged treatments^[5].

The electrospinning technique, when associated with synthetic polymers such as polyvinyl alcohol (PVA) and natural polymers such as bacterial cellulose biopolymer, results in biocompatible and biodegradable nanofibers with broad biomedical potential^[6]. PVA is a semi-crystalline hydrophilic, biocompatible, non-toxic polymer with remarkable chemical and thermal stability that favors the polymer in multiple medical, cosmetic, food, and pharmaceutical applications^[7].

Electrospun nanofibers, with their high surface area and structural similarity to the extracellular matrix (ECM), provide an ideal platform for wound healing applications^[8]. Mimicking the ECM architecture with a nanometer scale of 50-500 nm in diameter, these nanofibers offer a biomimetic environment that promotes cell adhesion, migration, and tissue regeneration^[6]. As healing dressings, electrospun nanofibers facilitate efficient moisture management, enhance drug delivery, and accelerate wound closure, making them promising candidates for advanced wound care solutions^[9].

The cellulosic biopolymer (BP), synthesized through the enzymatic action of the bacterium *Zoogloea* sp. on a sugarcane molasses substrate, demonstrates remarkable potential for biomedical applications^[10,11]. Cellulose is a linear homopolysaccharide composed of units of β -D-glucopyranose joined in long unbranched chains with β -glycosidic compounds (1 \rightarrow 4). This sustainable and bio-derived material offers versatility in drug delivery systems, tissue engineering, and wound healing due to its biocompatibility and unique mechanical properties. The synthesis process aligns with the growing demand for eco-friendly alternatives in the biomedical field^[12].

In recent decades, nanomaterials have attracted the interest of the biomedical industry due to their applications against various diseases. In this sense, silver nanoparticles (AgNPs) are among the most studied nanomaterials mainly due to their highly efficient antimicrobial characteristics^[13-16]. Their mechanism of antimicrobial action originated by binding to the negatively charged bacterial cell wall, causing subsequent destabilization of the cell envelope and alteration of the membrane permeability^[17].

The innate immune system has key components, such as antimicrobial peptides (AMPs), which form the first line of defense against pathogens. Clavanin A (ClavA) is an antimicrobial peptide (AMP) extracted from hemocytes of the tunicate of the invertebrate *Styela Clava*, revealed to be an excellent alternative against antimicrobial resistance^[18]. The association of the antimicrobial properties of the peptides with AgNPs yields a synergistic approach to combating infections and enhancing wound healing^[19]. Antimicrobial peptides exhibit broad-spectrum activity against bacteria, fungi, and viruses, while AgNPs provide sustained release of antimicrobial ions. Incorporating these components into healing dressings, such as electrospun nanofibers, creates a multifaceted solution that prevents infection and accelerates the healing process. Their synergistic action offers a promising avenue for developing advanced wound dressings with improved efficacy and reduced antibiotic resistance concerns^[20].

ESKAPE pathogens (*Enterococcus faecium*, *Staphylococcus aureus*, *Klebsiella pneumoniae*, *Acinetobacter baumannii*, *Pseudomonas aeruginosa*, and *Enterobacter species*) are frequently associated with infections. In addition, these species are known to be drug-resistant^[21]. Furthermore, damaged tissue from an injury can acquire infection caused by several bacterial species, such as *Pseudomonas spp.*, *Staphylococcus aureus*, *Klebsiella spp.*, *Escherichia coli*, and *Proteus spp.*^[22].

The present study focuses on the development, characterization, and evaluation of antimicrobial polymeric electrospun nanofibers based on polyvinyl alcohol (PVA), AgNPs, BP, and ClavA peptide. It focuses on antimicrobial activity against Gram-positive (*B. subtilis* and *S. aureus*) and Gram-negative (*K. pneumoniae*, *E. coli*, and *P. aeruginosa*) bacteria.

2. Materials and Methods

2.1 Reagents

Silver nitrate (AgNO₃), sodium borohydride (NaBH₄), potassium ferricyanide (K₃[Fe(CN)₆]), and potassium ferrocyanide (K₄[Fe(CN)₆]) were purchased from Sigma Aldrich (St. Louis, MO, USA). Polyvinyl alcohol (PVA) hydrolysis: Mol % = 87-89%; viscosity (20 °C, 4% CP) 40-48 and trisodium citrate were obtained from Dinâmica (Brazil). All chemicals were of analytical grade and used as received. Ultrapure water (18.2 Ω .cm⁻¹) used in the experiments was obtained using a Millipore Milli-Q plus purification system (Billerica, USA).

BP hydrogel from sugarcane molasses and synthesized by *Zoogloea* sp. through a flotation process^[23] was obtained by the Sugarcane Biopolymers Research Group (POLISA, Brazil - <https://www.polisa.ind.br>). Clavanin A (ClavA) peptide (amino acid sequence VFQFLGKIIHHVGNFVHGFSHFV-NH₂) was synthesized by Aminotech (São Paulo, Brazil) using the fluorenylmethoxycarbonyl (F-moc) technique, purified by high-performance liquid chromatography (purity > 95%) and lyophilized.

2.2 Preparation of PVA nanofibers hybrid composite membranes

Initially, 10% PVA was prepared in deionized water, remaining under constant stirring for 2h at 80 °C until a homogeneous solution was obtained. After that, the solution passes through an ultrasonic bath to remove bubbles. Then, the solution was poured into a 25 mL syringe with a metal needle (gauge 18) at room temperature. The needle was fixed at a distance of 15 cm from a grounded collector plate covered with aluminum foil. A voltage of 24 kV was applied to the polymer solution through an electrode connected to the needle. In addition, a fixed flow rate of 0.75 μ L.min⁻¹ was used.

The electrospinning process was carried out for ~5h. After, the fiber was removed from the collector and dried in air. Finally, the fibers were subjected to chemical crosslinking in a solution containing glutaraldehyde and hydrochloric acid^[24]. After 5 min, the nanofibers were washed thoroughly

with deionized water. After drying, the nanofibers were stored at 5 °C until use.

2.3 Synthesis of AgNPs

AgNPs were prepared according to Acharya et al.^[25] with some modifications. NaBH₄ and tri-sodium citrate were used as reducing and stabilizing agents, respectively. Initially, the nanofibers were cut (1 × 1 cm²) and inserted into a beaker containing 10 mL of 1 mM AgNO₃ and 0.5 mM tri-sodium citrate and were then subjected to magnetic stirring for 30 min. Then, 1 mL NaBH₄ (2 mM) was dripped into the solution, which immediately changed color, indicating the formation of nanoparticles impregnated into the fiber structure. The solution remained stirring for another 30 min. Finally, the fibers were washed three times in deionized water, dried, and stored.

2.4 Functionalization of nanofibers with BP and Clav

The functionalization of the nanofibers was carried out through absorption, with 1 mL of BP applied to each disc, and the remaining submerged for 1 hour, then the excess was removed. Peptide incorporation was achieved by adding 10 µL of Clav A peptide (100 µM) to each disc.

2.5 Characterization

Scanning electron microscopy (SEM) was performed using a Tescan MIRA3 microscope 200 V - 30 kV (Czech Republic). The nanofibers were deposited on a sheet and placed directly on a double-sided carbon tape fixed to the sample port. To obtain SEM images, a thin layer of gold was deposited over the samples using an SC-701 Quick Coater metallizer (Sanyu, USA). The diameter distribution of the nanofibers was obtained using ImageJ software. Histograms were prepared using OriginPro9.

Differential scanning calorimetry (DSC) curves were obtained using a calorimeter model DSC-50 (Shimadzu®) at a heating rate of 20 °C.min⁻¹. The experiments were performed under a dynamic nitrogen atmosphere (50 mL.min⁻¹), and a temperature range from 25 °C to 250 °C. The tests were carried out using a sample mass of 2.00 ± 0.10 mg in closed aluminum crucibles. Blank curves were obtained to evaluate the system's baseline. Indium metal (T_{fusion} = 156.6 °C; Δ_{fusion} = 28.7 J.g⁻¹) with a purity of 99.99% was used for DSC cell calibration.

Fourier Transform Infrared Spectroscopy (FTIR) measurements were performed using an Agilent Cary 630 FTIR spectrometer (Agilent Technologies, Australia) connected to a diamond-attenuated total reflectance (ATR) sampling accessory. Spectra were recorded between 1.000-4.000 cm⁻¹ with a resolution of 2 cm⁻¹.

For electrochemical analysis, the samples were immobilized in a corrosion cell, with the nanofiber as the working electrode, Ag/AgCl saturated with 3M KCl as the reference electrode, and platinum wire as the auxiliary counter electrode. The electrodes were immersed in the electrochemical cell containing a solution of 10 mM K₄[Fe(CN)₆]/K₃[Fe(CN)₆] (1:1, v/v) in phosphate buffer (PBS, pH 7.4), used as a redox probe. The experiments were carried out inside a Faraday cage. Square Wave Voltammetry (SWV) was performed

with a sweep potential between 0 V and 1.2 V with a sweep rate of 50 mV.s⁻¹, step potential 0.010 V, amplitude 0.025 V, and frequency 5 Hz.

2.6 Antimicrobial activity assay

The antimicrobial activity was evaluated against *S. aureus* ATCC 25923, *K. pneumoniae* ATCC 700603, *P. aeruginosa* ATCC 27853, *E. coli* ATCC 35218, and *B. subtilis* ATCC 6633, the inoculum concentration being used is 10⁸ cells.mL⁻¹. The antibiotics used in the control discs were gentamicin 10µg for gram-positive bacteria, meropenem 10µg for gram-negative bacteria, and 300µg polymyxin. The inhibition zones were evaluated by the disk diffusion method^[26]. Initially, the bacterial inoculum was distributed on the surface of Mueller-Hinton Agar and allowed to rest for 3 min. After, the nanofibers were cut into discs and equally distributed on the plate surface, which were incubated at 35 ± 1 °C for 24 h. The growth inhibition halo was measured using a millimeter ruler, and unmodified nanofiber disks were used as a control.

3. Results and Discussions

3.1 ATR-FTIR analyses

Figure 1 shows the ATR-FTIR of pure PVA and its mixtures with BP, Ag, and ClavA peptide. The spectrum of pure PVA electrospun nanofibers exhibited bands of O-H stretching vibrations at 3332 cm⁻¹ and C-H stretching vibrations at 2925 cm⁻¹ [26]. A particularity is the existence of close absorption bands at 1740 cm⁻¹ for PVA and 1718 cm⁻¹ for PVA-BP fibers that are generally associated with the stretching vibration of CO carbonyl groups of PVA chains^[27]. The increase in the concentration of the other components results in a PVA peak decrease, such as occurring at 1435 cm⁻¹ to 1425 cm⁻¹ in the PVA-BP fibers. Also, a decrease in the intensity of the 840 cm⁻¹ peak of the sample containing PVA to 820 cm⁻¹ corresponding to PVA-BP-Ag-ClavA samples^[28].

An intense absorption band was observed at 1376 cm⁻¹, associated with the presence of the Ag+NO₃ ion. The vibration

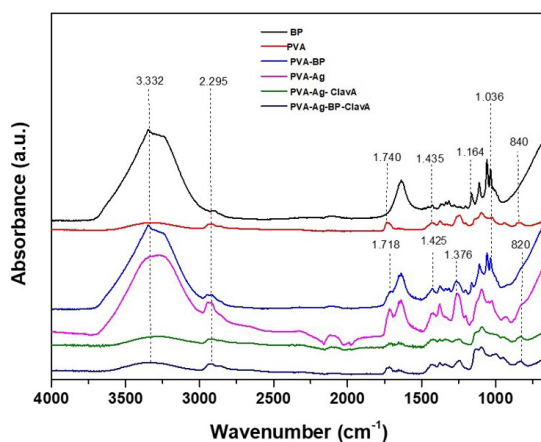


Figure 1. ATR-FTIR spectra of the tested samples at wavenumbers ranging from 4.000 cm⁻¹ to 1.000 cm⁻¹.

peak detected at 1164 cm^{-1} in samples containing the biopolymer is related to the bending vibration of the C-H and C-O bonds in the aromatic rings of polysaccharides^[29].

The peak at 1036 cm^{-1} can be attributed to the C-O-C and C-O-H stretching vibration of the sugar ring^[30].

3.2 SEM analysis

The morphology of the synthesized nanofibers (Figure 2) was analyzed by SEM (Figure 3). The micrographs showed that the nanofibers in different compositions formed a homogeneous three-dimensional matrix. Agglomerates were not observed for all samples^[31]. Figure 3 shows SEM images and histograms with the diameter distributions corresponding to the functionalized PVA nanofibers. As expected, the average diameters of the nanofibers varied slightly. The PVA nanofibers had a diameter of 568 nm, while the PVA-Ag nanofibers had the largest diameter measuring 648 nm. The morphology of the AgNPs-containing nanofiber (Figure 3B) shows surface changes suggesting the incorporation of the particles^[32].

The images obtained from energy dispersive X-ray spectroscopy (Figure 4) demonstrated the distribution of AgNPs in the nanofibers.

The EDS spectrum presents the elemental analysis of carbon and oxygen peaks corresponding to their binding energies. As predicted, cellulose mainly contains carbon, oxygen, and hydrogen^[29]. Elemental mapping revealed the homogeneous dispersion of silver nanoparticles on the surface of the nanofibers^[33].

3.3 DSC analysis

PVA nanofibers favor a decrease in the melting peak due to morphological modification^[34]. The thermal behavior of the samples was investigated by measuring endothermic melting events (Figure 5).

The highest melting peak of PVA-Ag-Bp-ClavA nanofibers was $207.03\text{ }^{\circ}\text{C}$. A similar melting temperature was previously found in a study on the preparation and characterization of PVA microfibers associated with titanium dioxide, where thermograms of the synthesized fibers indicated the melting temperature at $223.7\text{ }^{\circ}\text{C}$ ^[35]. Another

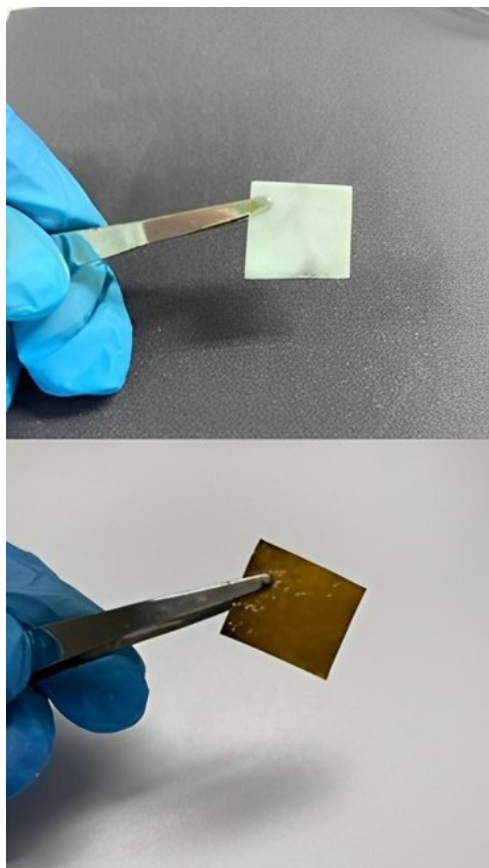


Figure 2. PVA nanofibers functionalized with Ag-BP-ClavA.

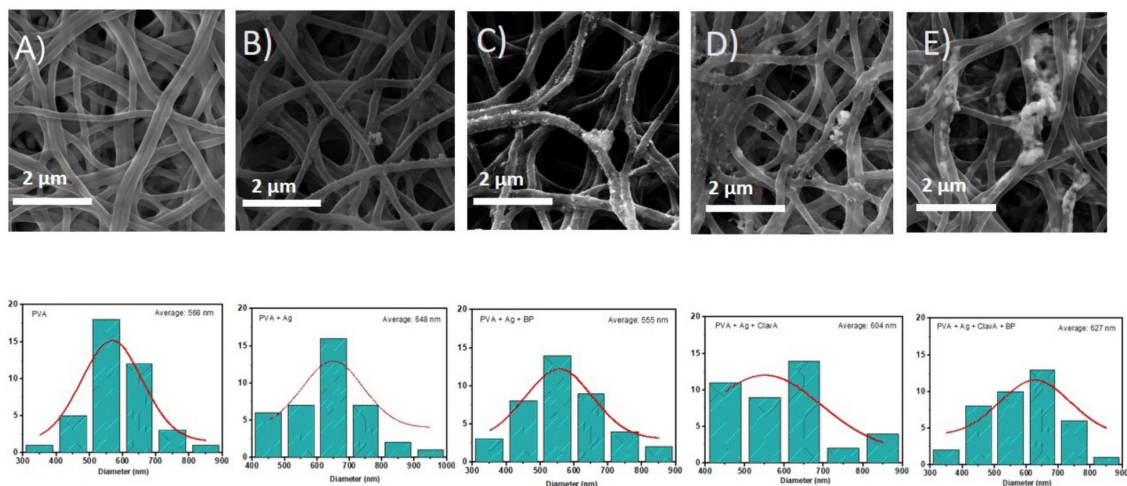


Figure 3. Scanning electron microscopy of the tested samples, as follow: (A) PVA; (B) PVA-Ag; (C) PVA-Ag-ClavA; (D) PVA-Ag-BP; (E) PVA-Ag-BP-ClavA.

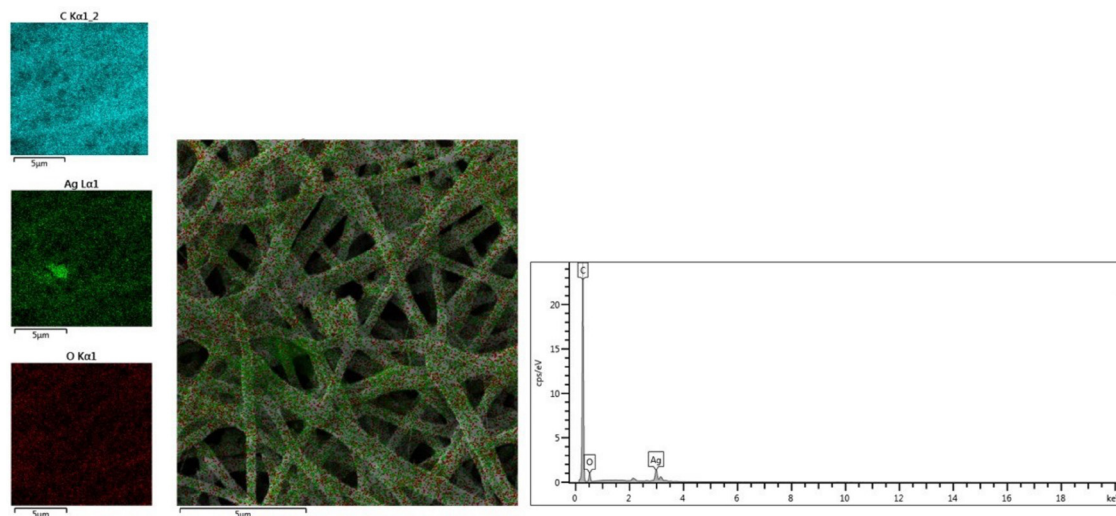


Figure 4. X-ray energy dispersive spectroscopy (EDS) of PVA-Ag-BP nanofibers shows the main chemical elements identified in the sample: C (blue), Ag (green), and O (red). On the right, the elemental map and its respective energy peaks are shown.

study developed electrospun nanofibers with cephalexin prepared from PVA associated with different biopolymers presented a melting temperature of pure PVA nanofibers of 176.50 °C; when associated with carboxymethylcellulose, there was an increase in the temperature of melting to 195.47 °C^[31]. A previous study that evaluated the thermal behavior of PVA showed a similar result, with a peak melting temperature of 189 °C^[36]. The melting peak of pure PVA nanofibers was 130.92 °C since the presentation of nanofibers favors a decrease in the melting peak due to morphological modification and is associated with changes resulting from crosslinking^[34]. According to the melting peak value of the sample containing BP, Ag, and ClavA, it is evident that the thermal stability was significantly higher than that of pure PVA. The increase in thermostability from 130.92 °C to 207.03 °C may be caused by the formation of hydrogen bonds between PVA and the biopolymer^[31].

3.4 Electrochemical measurements

The electrochemical behavior of PVA, Ag, and BP-embedded nanofibers was studied. SWV technique provided values related to surface modification, facilitating the monitoring of current responses as a function of the applied potential and allowing the characterization of the sample's charge transfer rates^[37]. PVA nanofibers have insulating properties^[36]. PVA nanofibers have improved electron transport properties when associated with metal nanoparticles^[38]. The modifications of the PVA fibers with Ag and BP showed increased peaks (Figure 6), indicating a greater concentration or activity of redox species.

A recent study showed that the electrical conductivity of bacterial cellulose increases when associated with metal nanoparticles^[39].

After adding the compounds to the fibers, the degree of interaction can be evaluated through the percentage of relative deviation of the anodic current variation ΔI , using the following Equation 1^[40,41]:

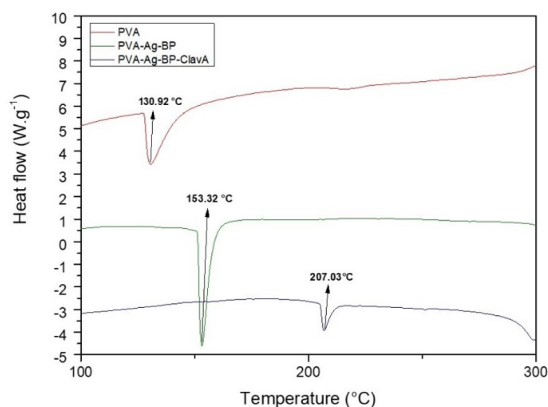


Figure 5. Thermal analysis of the PVA, PVA-Ag, PVA-Ag-BP, and PVA-Ag-BP-ClavA.

$$\Delta I(\%) = \frac{\left[\left(\frac{1}{I_b} \right) - \left(\frac{1}{I_a} \right) \right]}{\left(\frac{1}{I_b} \right)} \times 100 \quad (1)$$

Table 1 shows the ΔI results for the studied systems. ΔI values revealed an increase in the peak current of fibers containing Ag and BP, when compared to PVA nanofibers.

3.5 Antimicrobial activity

The antimicrobial activity of the pure PVA fiber and functionalized nanofibers was investigated against Gram-positive and Gram-negative bacteria using the disc diffusion method. The results are shown in Figure 7 and summarized in Table 2. PVA fiber did not reveal inhibitory activity against all microorganisms evaluated. On the other hand, functionalized nanofibers showed significant antibacterial

activity. The nanofibers composed of PVA-Ag, PVA-Ag-ClavA, and PVA-Ag-BP showed satisfactory inhibitory action against gram-positive bacteria (*S. aureus* and *B. subtilis*). There was a formation of an inhibition zone for *P. aeruginosa*, with a larger halo of 15mm for PVA-Ag, PVA-Ag-ClavA, and PVA-Ag-BP-ClavA systems. In addition, PVA-Ag-BP showed a halo of 13mm against *S. aureus* and 12mm for *B. subtilis*.

PVA-Ag and PVA-Ag-BP-ClavA demonstrated inhibitory activity against *K. pneumoniae*. Of note, the most common

bacterial species in sepsis are *S. aureus* (30% of cases, 14% of which are methicillin-resistant) and *Pseudomonas spp.* (14% of cases)^[42]. Of note, the antimicrobial action of AgNPs is linked to the surface area of the nanomaterial. The highest concentrations of Ag⁺ ions released were identified in AgNPs with greater surface area. Favorably, the low release of Ag⁺ ions was found for AgNPs with low surface area, resulting in failures of antimicrobial characteristics^[43]. It is well known that cellulose compounds utilized to functionalize the AgNPs-impregnated PVA nanofiber are poorly soluble in agar and water. On the other hand, AgNPs coated in substances that dissolve in water demonstrate advantageous antibacterial properties. It is worth mentioning that bacterial cellulose acts as a physical barrier to prevent infections but does not have any antibacterial features. Therefore, adding recognized bacteriostatic and bactericidal substances to surfaces, like AgNPs and antimicrobial peptides, enables the BC to exhibit antimicrobial activity as therapeutic materials. Thus, these agents were adsorbed by BP matrices due to their large surface area and the presence of hydroxyl groups that can interact chemically and intermolecularly^[44,45].

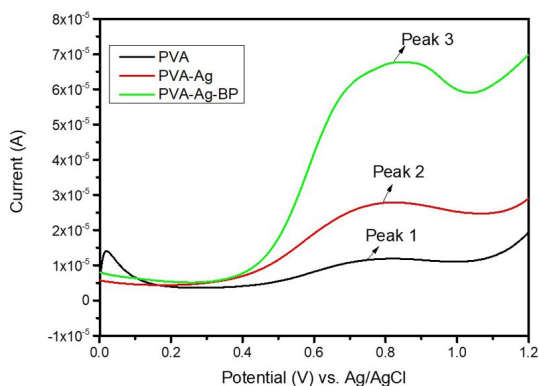


Figure 6. The electrochemical behavior of the PVA, PVA-Ag, and PVA-Ag-BP using square wave voltammetry.

Table 1. Variation in the anodic current (iPA) of the nanofibers.

Samples	iPA (μA)	Δi
PVA	3.56	
PVA-Ag	11.06	-202.41%
PVA-Ag-BP	21.029	-744.87

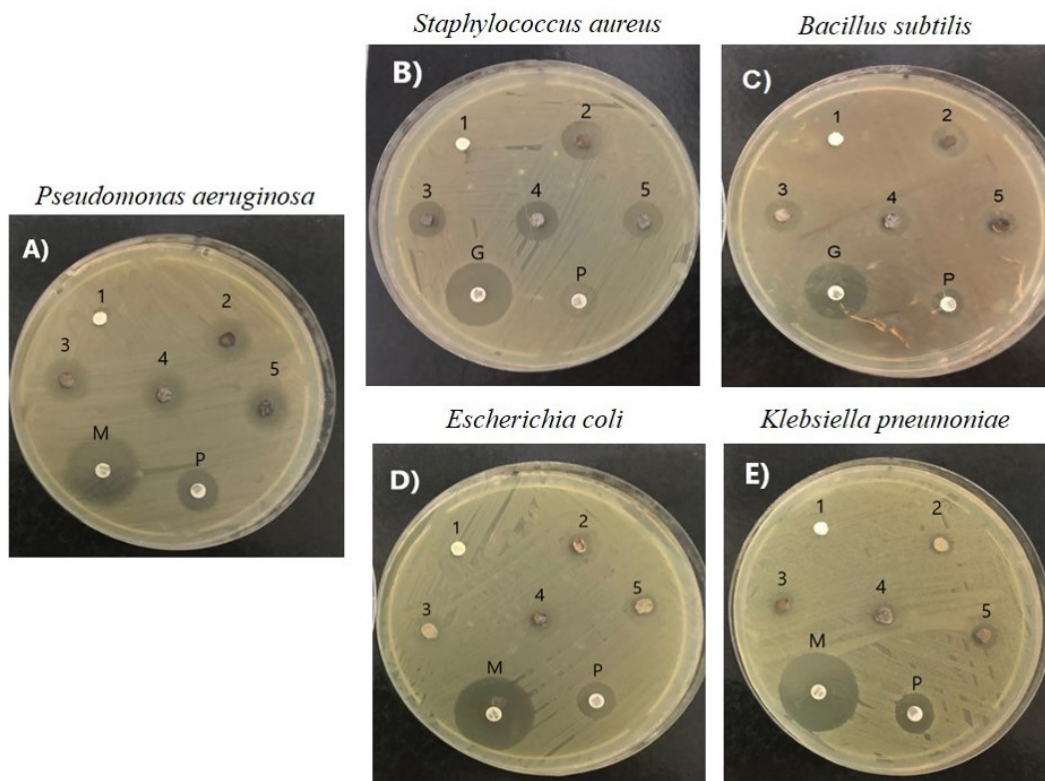


Figure 7. Inhibitory halos against bacteria, represented by (1) PVA; (2) PVA-Ag; (3) PVA-Ag-ClavA; (4) PVA-Ag-BP; (5) PVA-Ag-BP-ClavA; G = Gentamicin; P = Polymyxin B; M = Meropenem.

Table 2. Evaluation of the antibacterial activity of the nanofibers, as follows: absence of inhibition halo PVA, PVA-Ag, PVA-Ag-ClavA, PVA-Ag-BP, PVA-Ag-BP-ClavA, Gentamicin (letter G), Polymyxin B (letter P), Meropenem (letter M), and not applicable (-).

Sample	Microorganisms			
	<i>Staphylococcus aureus</i> ATCC 25923	<i>Pseudomonas aeruginosa</i> ATCC 27853	<i>Klebsiella pneumoniae</i> ATCC 700603	<i>Bacillus subtilis</i> ATCC 6333
PVA	0	0	0	0
PVA-Ag	13mm	15mm	8mm	12mm
PVA-Ag-Clav A	13mm	15 mm	0	12mm
PVA-Ag-BP	13mm	14mm	0	12mm
PVA-Ag-BP-ClavA	12mm	15mm	8mm	10mm
G	20mm	-	-	17mm
M	30mm	28mm	30mm	
P	-	14mm	13mm	11mm

Subtitle: 0 = absence of inhibition halo; G = Gentamicin; P = Polymyxin B; M = Meropenem; (-) = Not applicable.

No significant results were obtained for *E. coli*. The low antibacterial activity against *E. coli* can be justified by the presence of lipopolysaccharides that defend against antibacterial agents^[46]. Gopiraman et al.^[34] Investigating the antimicrobial activity of anionic cellulose nanofiber composites coated with silver revealed an absence of halo formation in the studied samples.

Clavanin A is highly effective against Gram-positive bacteria, such as methicillin-resistant *Staphylococcus aureus*, Gram-negative bacteria and fungi^[42]. However, in this study, there was no significant increase in the antibacterial action of the nanofibers functionalized with the peptide; there was a slight increase in the inhibition halo for *Pseudomonas aeruginosa*.

4. Conclusions

This study presents a new and eco-friendly alternative for preparing nanofibers with antimicrobial activity based on PVA associated with BP obtained from sugar cane molasses. AgNPs and ClavA peptide were effectively incorporated into the polymeric nanofibers. Modified nanofibers revealed electrical variation with the increase in charge transfer. The nanofibers showed inhibitory activity against microorganisms frequently associated with wound infections such as *B. subtilis*, *S. aureus*, *P. aeruginosa*, and *K. pneumoniae*. Nanofibers containing ClavA peptide were more effective against *P. aeruginosa*. The developed nanofibers stand out as potential candidates in the biomedical field, such as wound dressings and surgical instrumentation coatings, environments known to be favorable for the colonization of microorganisms.

5. Author's Contribution

- **Conceptualization** – Glícia Maria Oliveira; César Augusto Souza de Andrade.
- **Data curation** – Glícia Maria Oliveira; Alberto Galdino Silva-Junior.
- **Formal analysis** – César Augusto Souza de Andrade, Maria Danielly Lima de Oliveira
- **Funding acquisition** – César Augusto Souza de Andrade; Maria Danielly Lima de Oliveira.

• **Investigation** – Glícia Maria Oliveira; Alberto Galdino Silva-Junior.

• **Methodology** – César Augusto Souza de Andrade; Maria Danielly Lima de Oliveira; Alberto Galdino Silva-Junior; Octávio Luiz Franco; José Lamartine de Andrade Aguiar; Flávia Cristina Morone Pinto; Reginaldo Gonçalves de Lima-Neto.

• **Project administration** – César Augusto Souza de Andrade; Maria Danielly Lima de Oliveira.

• **Resources** – César Augusto Souza de Andrade; Octávio Luiz Franco; José Lamartine de Andrade Aguiar; Flávia Cristina Morone Pinto; Reginaldo Gonçalves de Lima-Neto.

• **Software** – NA.

• **Supervision** – César Augusto Souza de Andrade.

• **Validation** – César Augusto Souza de Andrade; Maria Danielly Lima de Oliveira; Alberto Galdino Silva-Junior.

• **Visualization** – César Augusto Souza de Andrade; Maria Danielly Lima de Oliveira; Alberto Galdino Silva-Junior.

• **Writing – original draft** – Glícia Maria de Oliveira.

• **Writing – review & editing** – César Augusto Souza de Andrade; Maria Danielly Lima de Oliveira; Alberto Galdino Silva-Junior.

6. Acknowledgements

The authors are grateful for the support from the Coordination for the FACEPE and the Brazilian National Council of Scientific and Technological Development/CNPq (grant numbers 304678/2021-0 and 304680/2021-4).

7. References

1. Caldwell, M. D. (2020). Bacteria and antibiotics in wound healing. *The Surgical Clinics of North America*, 100(4), 757-776. <http://doi.org/10.1016/j.suc.2020.05.007>. PMID:32681875.
2. Sen, C. K., Gordillo, G. M., Roy, S., Kirsner, R., Lambert, L., Hunt, T. K., Gottrup, F., Gurtner, G. C., & Longaker, M. T. (2009). Human skin wounds: a major and snowballing threat to public health and the economy. *Wound Repair and Regeneration*, 17(6), 763-771. <http://doi.org/10.1111/j.1524-475X.2009.00543.x>. PMID:19903300.

3. Hurlow, J., & Bowler, P. G. (2022). Acute and chronic wound infections: microbiological, immunological, clinical and therapeutic distinctions. *Journal of Wound Care*, 31(5), 436-445. <http://doi.org/10.12968/jowc.2022.31.5.436>. PMID:35579319.
4. Shalaby, M. A., Anwar, M. M., & Saeed, H. (2022). Nanomaterials for application in wound healing: current state-of-the-art and future perspectives. *Journal of Polymer Research*, 29(3), 91. <http://doi.org/10.1007/s10965-021-02870-x>.
5. Kolimi, P., Narala, S., Nyavanandi, D., Yousef, A. A. A., & Dudhipala, N. (2022). (Year). Innovative treatment strategies to accelerate wound healing: trajectory and recent advancements. *Cells*, 11(15), 2439. <http://doi.org/10.3390/cells11152439>. PMID:35954282.
6. Singh, B. K., & Dutta, P. K. (2015). *Chitin, chitosan, and silk fibroin electrospun nanofibrous scaffolds: A prospective approach for regenerative medicine*. In S. Kalia (Ed.), *Chitin and chitosan for regenerative medicine* (pp. 151-189). New Delhi: Springer. http://doi.org/10.1007/978-81-322-2511-9_7.
7. Zhang, W., Ronca, S., & Mele, E. (2017). Electrospun nanofibres containing antimicrobial plant extracts. *Nanomaterials*, 7(2), 42. <http://doi.org/10.3390/nano7020042>. PMID:28336874.
8. Gao, C., Zhang, L., Wang, J., Jin, M., Tang, Q., Chen, Z., Cheng, Y., Yang, R., & Zhao, G. (2021). Electrospun nanofibers promote wound healing: theories, techniques, and perspectives. *Journal of Materials Chemistry. B, Materials for Biology and Medicine*, 9(14), 3106-3130. <http://doi.org/10.1039/D1TB00067E>. PMID:33885618.
9. Nadaf, A., Gupta, A., Hasan, N., Fauziya, Ahmad, S., Kesharwani, P., & Ahmad, F. J. (2022). Recent update on electrospinning and electrospun nanofibers: current trends and their applications. *RSC Advances*, 12(37), 23808-23828. <http://doi.org/10.1039/D2RA02864F>. PMID:36093244.
10. Oliveira, G. M., Gomes, A. O., Fo., Silva, J. G. M., Silva, A. G., Jr., Lins, E. M., Oliveira, M. D. L., & Andrade, C. A. S. (2023). Bacterial cellulose biomaterials for the treatment of lower limb ulcers. *Revista do Colégio Brasileiro de Cirurgiões*, 50(1), e20233536. <http://doi.org/10.1590/0100-6991e-20233536-en>. PMID:37222383.
11. Silva, J. G. M., Pinto, F. C. M., Oliveira, G. M., Silva, A. A., Campos, O., Jr., Silva, R. O., Teixeira, V. W., Melo, I. M. F., Paumgarten, F. J. R., Souza, T. P., Carvalho, R. R., Oliveira, A. C. A. X., Aguiar, J. L. A., & Teixeira, Á. A. C. (2020). Non-clinical safety study of a sugarcane bacterial cellulose hydrogel. *Research, Society and Development*, 9(9), e960997932. <http://doi.org/10.33448/rsd-v9i9.7932>.
12. Pinto, F. C. M., De-Oliveira, A. C. A. X., De-Carvalho, R. R., Gomes-Carneiro, M. R., Coelho, D. R., Lima, S. V. C., Paumgarten, F. J. R., & Aguiar, J. L. A. (2016). Acute toxicity, cytotoxicity, genotoxicity and antigenotoxic effects of a cellulosic exopolysaccharide obtained from sugarcane molasses. *Carbohydrate Polymers*, 137, 556-560. <http://doi.org/10.1016/j.carbpol.2015.10.071>. PMID:26686163.
13. Gurunathan, S. (2019). Rapid biological synthesis of silver nanoparticles and their enhanced antibacterial effects against *Escherichia fergusonii* and *Streptococcus mutans*. *Arabian Journal of Chemistry*, 12(2), 168-180. <http://doi.org/10.1016/j.arabjc.2014.11.014>.
14. Behravan, M., Panahi, A. H., Naghizadeh, A., Ziaee, M., Mahdavi, R., & Mirzapour, A. (2019). Facile green synthesis of silver nanoparticles using *Berberis vulgaris* leaf and root aqueous extract and its antibacterial activity. *International Journal of Biological Macromolecules*, 124, 148-154. <http://doi.org/10.1016/j.ijbiomac.2018.11.101>. PMID:30447360.
15. Kalaivani, R., Maruthupandy, M., Muneeswaran, T., Hameedha Beevi, A., Anand, M., Ramakritinan, C. M., & Kumaraguru, A. K. (2018). Synthesis of chitosan mediated silver nanoparticles (Ag NPs) for potential antimicrobial applications. *Frontiers in Laboratory Medicine*, 2(1), 30-35. <http://doi.org/10.1016/j.flm.2018.04.002>.
16. Singh, H., Du, J., Singh, P., & Yi, T. H. (2018). Extracellular synthesis of silver nanoparticles by *Pseudomonas* sp. THG-LS1.4 and their antimicrobial application. *Journal of Pharmaceutical Analysis*, 8(4), 258-264. <http://doi.org/10.1016/j.jppha.2018.04.004>. PMID:30140490.
17. Guzmán, M. G., Dille, J., & Godet, S. (2009). Synthesis of silver nanoparticles by chemical reduction method and their antibacterial activity. *International Journal of Chemical and Biomolecular Engineering*, 2(3), 104-111.
18. Pasupuleti, M., Schmidtchen, A., & Malmsten, M. (2012). Antimicrobial peptides: key components of the innate immune system. *Critical Reviews in Biotechnology*, 32(2), 143-171. <http://doi.org/10.3109/07388551.2011.594423>. PMID:22074402.
19. Xu, J., Li, Y., Wang, H., Zhu, M., Feng, W., & Liang, G. (2021). Enhanced antibacterial and anti-biofilm activities of antimicrobial peptides modified silver nanoparticles. *International Journal of Nanomedicine*, 16, 4831-4846. <http://doi.org/10.2147/IJN.S315839>. PMID:34295158.
20. Browne, K., Chakraborty, S., Chen, R., Willcox, M. D., Black, D. S., Walsh, W. R., & Kumar, N. (2020). A new era of antibiotics: the clinical potential of antimicrobial peptides. *International Journal of Molecular Sciences*, 21(19), 7047. <http://doi.org/10.3390/ijms21197047>. PMID:32987946.
21. Santajit, S., & Indrawattana, N. (2016). Mechanisms of antimicrobial resistance in ESKAPE pathogens. *BioMed Research International*, 2016, 2475067. <http://doi.org/10.1155/2016/2475067>. PMID:27274985.
22. Kalan, L. R., & Brennan, M. B. (2019). The role of the microbiome in nonhealing diabetic wounds. *Annals of the New York Academy of Sciences*, 1435(1), 79-92. <http://doi.org/10.1111/nyas.13926>. PMID:30003536.
23. Paterson-Beedle, M., Kennedy, J. F., Melo, F. A. D., Lloyd, L. L., & Medeiros, V. (2000). A cellulosic exopolysaccharide produced from sugarcane molasses by a *Zoogloea* sp. *Carbohydrate Polymers*, 42(4), 375-383. [http://doi.org/10.1016/S0144-8617\(99\)00179-4](http://doi.org/10.1016/S0144-8617(99)00179-4).
24. Ullah, S., Hashmi, M., Hussain, N., Ullah, A., Sarwar, M. N., Saito, Y., Kim, S. H., & Kim, I. S. (2020). Stabilized nanofibers of polyvinyl alcohol (PVA) crosslinked by unique method for efficient removal of heavy metal ions. *Journal of Water Process Engineering*, 33, 101111. <http://doi.org/10.1016/j.jwpe.2019.101111>.
25. Acharya, D., Mohanta, B., Pandey, P., Singha, M., & Nasiri, F. (2017). Optical and antibacterial properties of synthesised silver nanoparticles. *Micro & Nano Letters*, 12(4), 223-226. <http://doi.org/10.1049/mnl.2016.0666>.
26. İspir, E., Toroğlu, S., & Kayraldız, A. (2008). Syntheses, characterization, antimicrobial and genotoxic activities of new Schiff bases and their complexes. *Transition Metal Chemistry*, 33(8), 953-960. <http://doi.org/10.1007/s11243-008-9135-2>.
27. Abdul Khalil, H. P. S., Davoudpour, Y., Islam, M. N., Mustapha, A., Sudesh, K., Dungani, R., & Jawaid, M. (2014). Production and modification of nanofibrillated cellulose using various mechanical processes: a review. *Carbohydrate Polymers*, 99, 649-665. <http://doi.org/10.1016/j.carbpol.2013.08.069>. PMID:24274556.
28. Qashou, S. I., El-Zaidia, E. F. M., Darwish, A. A. A., & Hanafy, T. A. (2019). Methylsilicon phthalocyanine hydroxide doped PVA films for optoelectronic applications: FTIR spectroscopy, electrical conductivity, linear and nonlinear optical studies. *Physica B, Condensed Matter*, 571, 93-100. <http://doi.org/10.1016/j.physb.2019.06.063>.

29. Bai, J., Li, Y., Yang, S., Du, J., Wang, S., Zheng, J., Wang, Y., Yang, Q., Chen, X., & Jing, X. (2007). A simple and effective route for the preparation of poly(vinylalcohol) (PVA) nanofibers containing gold nanoparticles by electrospinning method. *Solid State Communications*, 141(5), 292-295. <http://doi.org/10.1016/j.ssc.2006.10.024>.
30. Sofla, M. R. K., Brown, R. J., Tsuzuki, T., & Rainey, T. J. (2016). A comparison of cellulose nanocrystals and cellulose nanofibres extracted from bagasse using acid and ball milling methods. *Advances in Natural Sciences: Nanoscience and Nanotechnology*, 7(3), 035004. <http://doi.org/10.1088/2043-6262/7/3/035004>.
31. Ghozali, M., Meliana, Y., & Chalid, M. (2021). Synthesis and characterization of bacterial cellulose by Acetobacter xylinum using liquid tapioca waste. *Materials Today: Proceedings*, 44(Part 1), 2131-2134. <http://doi.org/10.1016/j.matpr.2020.12.274>.
32. Hameed, M. M. A., Khan, S. A. P. M., Thamer, B. M., Al-Enizi, A., Aldalbahi, A., El-Hamshary, H., & El-Newehy, M. H. (2021). Core-shell nanofibers from poly(vinyl alcohol) based biopolymers using emulsion electrospinning as drug delivery system for cephalixin drug. *Journal of Macromolecular Science, Part A: Pure and Applied Chemistry*, 58(2), 130-144. <http://doi.org/10.1080/10601325.2020.1832517>.
33. Nasikhudin, D., Diantoro, M., Kusumaatmaja, A., & Triyana, K. (2016). Preparation of PVA/Chitosan/TiO₂ nanofibers using electrospinning method. *AIP Conference Proceedings*, 1755(1), 150002. <http://doi.org/10.1063/1.4958575>.
34. Gopiraman, M., Deng, D., Saravanamoorthy, S., Chung, I.-M., & Kim, I. S. (2018). Gold, silver and nickel nanoparticle anchored cellulose nanofiber composites as highly active catalysts for the rapid and selective reduction of nitrophenols in water. *RSC Advances*, 8(6), 3014-3023. <http://doi.org/10.1039/C7RA10489H>. PMID:35541203.
35. Blanes, M., Gisbert, M. J., Marco, B., Bonet, M., Gisbert, J., & Balart, R. (2010). Influence of glyoxal in the physical characterization of PVA nanofibers. *Textile Research Journal*, 80(14), 1465-1472. <http://doi.org/10.1177/0040517509357654>.
36. Oliveira, A. H. P., Moura, J. A. S., & Oliveira, H. P. (2013). Preparação e caracterização de microfibras de poli(álcool vinílico)/dióxido de titânio. *Polímeros: Ciência e Tecnologia*, 23(2), 196-200. <http://doi.org/10.1590/S0104-14282013005000013>.
37. van Etten, E. A., Ximenes, E. S., Tarasconi, L. T., Garcia, I. T. S., Forte, M. M. C., & Boudinov, H. (2014). Insulating characteristics of polyvinyl alcohol for integrated electronics. *Thin Solid Films*, 568, 111-116. <http://doi.org/10.1016/j.tsf.2014.07.051>.
38. Abeykoon, S. W., & White, R. J. (2022). Continuous square wave voltammetry for high information content interrogation of conformation switching sensors. *ACS Measurement Science*, 3(1), 1-9. <http://doi.org/10.1021/acsmesuresci.2c00044>. PMID:36817008.
39. Katouah, H. A., El-Sayed, R., & El-Metwaly, N. M. (2021). Solution blowing spinning technology and plasma-assisted oxidation-reduction process toward green development of electrically conductive cellulose nanofibers. *Environmental Science and Pollution Research International*, 28(40), 56363-56375. <http://doi.org/10.1007/s11356-021-14615-w>. PMID:34050912.
40. Khamwongsa, P., Wongjom, P., Cheng, H., Lin, C. C., & Ummartyotin, S. (2022). Significant enhancement of electrical conductivity of conductive cellulose derived from bamboo and polypyrrole. *Composites Part C: Open Access*, 9, 100314. <http://doi.org/10.1016/j.jcomc.2022.100314>.
41. Meirinho, S. G., Dias, L. G., Peres, A. M., & Rodrigues, L. R. (2017). Electrochemical aptasensor for human osteopontin detection using a DNA aptamer selected by SELEX. *Analytica Chimica Acta*, 987, 25-37. <http://doi.org/10.1016/j.aca.2017.07.071>. PMID:28916037.
42. Miranda, J. L., Oliveira, M. D. L., Oliveira, I. S., Frias, I. A. M., Franco, O. L., & Andrade, C. A. S. (2017). A simple nanostructured biosensor based on clavainin A antimicrobial peptide for gram-negative bacteria detection. *Biochemical Engineering Journal*, 124, 108-114. <http://doi.org/10.1016/j.bej.2017.04.013>.
43. Silva, O. N., Fensterseifer, I. C. M., Rodrigues, E. A., Holanda, H. H. S., Novaes, N. R. F., Cunha, J. P. A., Rezende, T. M. B., Magalhães, K. G., Moreno, S. E., Jerônimo, M. S., Bocca, A. L., & Franco, O. L. (2015). Clavainin A improves outcome of complications from different bacterial infections. *Antimicrobial Agents and Chemotherapy*, 59(3), 1620-1626. <http://doi.org/10.1128/AAC.03732-14>. PMID:25547358.
44. Villarreal-Gómez, L. J., Pérez-González, G. L., Bogdanchikova, N., Pestryakov, A., Nimaev, V., Soloveva, A., Cornejo-Bravo, J. M., & Toledoño-Magaña, Y. (2021). Antimicrobial effect of electrospun nanofibers loaded with silver nanoparticles: influence of Ag incorporation method. *Journal of Nanomaterials*, 2021, e9920755. <http://doi.org/10.1155/2021/9920755>.
45. Gromovykh, T. I., Vasil'kov, A. Yu., Sadykova, V. S., Feldman, N. B., Demchenko, A. G., Lyundup, A. V., Butenko, I. E., & Lutsenko, S. V. (2019). Creation of composites of bacterial cellulose and silver nanoparticles: evaluation of antimicrobial activity and cytotoxicity. *International Journal of Nanotechnology*, 16(6-10), 408-420. <http://doi.org/10.1504/IJNT.2019.106615>.
46. Garza-Cervantes, J. A., Mendiola-Garza, G., Macedo de Melo, E., Dugmore, T. I. J., Matharu, A. S., & Morones-Ramirez, J. R. (2020). Antimicrobial activity of a silver-microfibrillated cellulose biocomposite against susceptible and resistant bacteria. *Scientific Reports*, 10(1), 7281. <http://doi.org/10.1038/s41598-020-64127-9>. PMID:32350328.

Received: Mar. 20, 2024

Revised: Jul. 08, 2024

Accepted: Jul. 17, 2024